Apparatus for measuring local stress of metallic films, using an array of parallel laser beams during rapid thermal processing

2010 Meas. Sci. Technol. 21 055702

(http://iopscience.iop.org/0957-0233/21/5/055702)

Meas. Sci. Technol. **21** (2010) 055702 (9pp) doi:10.1088/0957-0233/21/5/055702

Apparatus for measuring local stress of metallic films, using an array of parallel laser beams during rapid thermal processing

R Huang[1,2], C A Taylor[3], S Himmelsbach[4], H Ceric[2] and T Detzel[5]

[1] Kompetenzzentrum Automobil-und Industrieelektronik (KAI) GmbH, Europastrasse 8, 9500 Villach, Austria
[2] Institute for Microelectronics, TU Vienna, Gusshausstrasse 27-29, 1040 Vienna, Austria
[3] k-Space Associates Inc., 2182 Bishop Circle East, Dexter, MI 48130, USA
[4] UniTemp GmbH, Senefelder Strasse 9, 85276 Pfaffenhofen/Ilm, Germany
[5] Infineon Technologies Austria AG, Siemensstrasse 2, 9500 Villach, Austria

Received 12 July 2009, in final form 8 February 2010
Published 26 March 2010
Online at stacks.iop.org/MST/21/055702

Abstract
The novel apparatus described here was developed to investigate the thermo-mechanical behavior of metallic films on a substrate by acquiring the wafer curvature. It comprises an optical module producing and measuring an array of parallel laser beams, a high resolution scanning stage, a rapid thermal processing (RTP) chamber and several accessorial gas control modules. Unlike most traditional systems which only calculate the average wafer curvature, this system has the capability to measure the curvature locally in 30 ms. Consequently, the real-time development of biaxial stress involved in thin films can be fully captured during any thermal treatments such as temperature cycling or annealing processes. In addition, the multiple parallel laser beam technique cancels electrical, vibrational and other random noise sources that would otherwise make an *in situ* measurement very difficult. Furthermore, other advanced features such as the *in situ* acid treatment and active cooling extend the experimental conditions to provide new insights into thin film properties and material behavior.

Keywords: curvature measurement, parallel laser beams, rapid thermal processing, local stress

(Some figures in this article are in colour only in the electronic version)

1. Introduction

Thermally induced stress in thin films is one of the most critical factors that may lead to cracks, voids, delamination or other failure modes in semiconductor devices [1–3]. The stress evolution during temperature cycling characterizes film properties, e.g. elastic modulus, coefficient of thermal expansion and temperature-dependent yield stress. Moreover, plastic deformation mechanisms such as dislocation glide/climb and diffusion can be investigated by stress measurement during temperature cycling. The creep behavior of thin films can be studied by recording stress relaxation at stabilized temperatures. Therefore, the fundamental understanding of thin films in terms of thermally induced stress and rate-dependent stress changes is of great importance in order to enhance the reliability and stability of semiconductor devices.

There are a variety of methods to determine the stress in thin films. X-ray diffraction is one of the most informative ways [3, 4], because it permits the local measurement of all the components of stress in the film. However, it is limited to crystalline films due to its diffraction-based technique. With the grid reflection method [5, 6], e.g. moiré pattern, stress measurements can be extended to noncrystalline films such

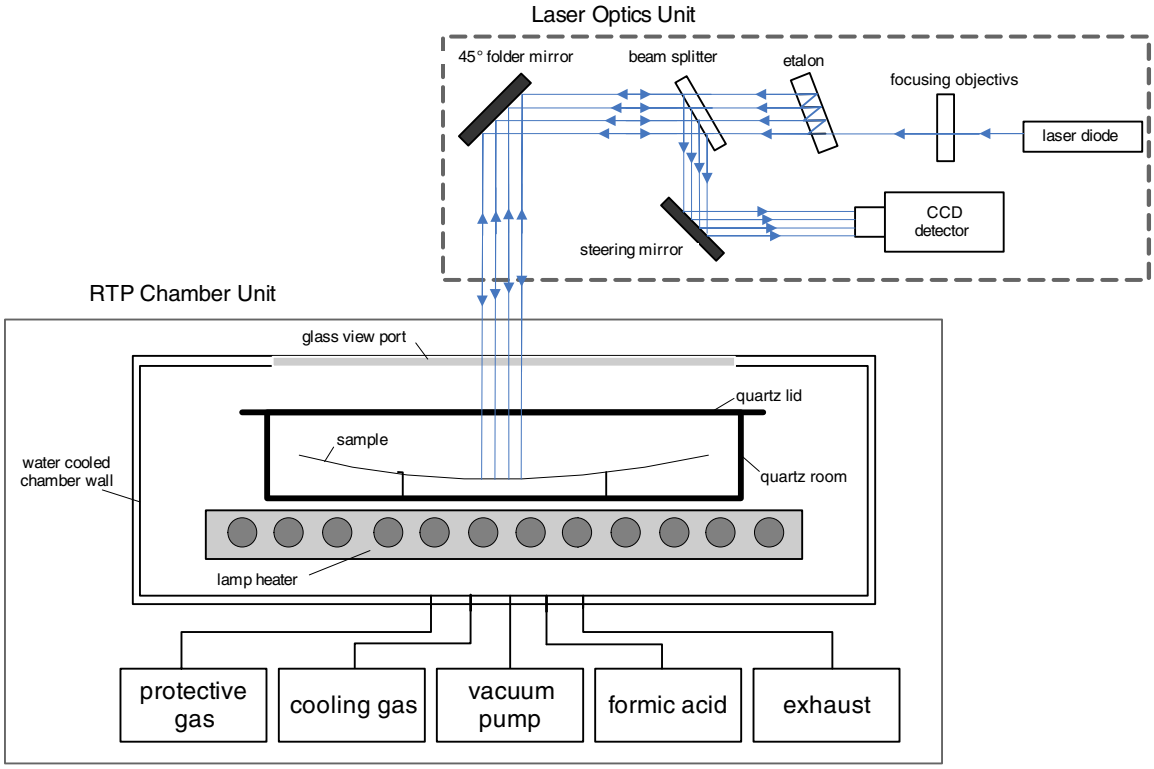

Figure 1. Scheme of the apparatus for film stress measurements with multiple laser beams integrated with a RTP chamber. The paths of the multiple laser beams for the wafer curvature detection are indicated.

as passivation glasses or amorphous oxides. However, this full-field measurement requires a large surface area in order to capture a decent pattern and consequently the local stress in the thin film is difficult to acquire. The wafer curvature technique is one of the most common methods. However, traditional single laser beam scanning cannot detect the wafer curvature directly. Instead, it measures the tilt and calculates differential bow height from point to point. For small deformations, bow height is related to curvature through the following equation:

$$\frac{1}{R} \approx \frac{2B}{x^2}, \tag{1}$$

where R is the radii of curvature, B is the measured bow height and x is the scan step size. The measurement accuracy highly depends on the scan length and the number of measurement points. Usually, only the global average stress in the film can be acquired. Furthermore, this technique is also dependent on and thus limited by the time span of the laser scanning. In the case of fast temperature ramping rate, e.g. $\geqslant 0.5\ ^{\circ}\mathrm{C\ s^{-1}}$, the scanning takes too long to acquire enough data and therefore the accuracy is questionable.

By measuring the curvature change of a wafer substrate before and after film deposition (R_0 and R_1, the initial and final radii of curvature, respectively), the stress involved in the film can be calculated by Stoney's equation, in principle [3, 7], if the film is much thinner than the substrate:

$$\sigma = \frac{Eh^2}{(1-\nu)6t}\left(\frac{1}{R_1} - \frac{1}{R_0}\right), \tag{2}$$

where σ is the film stress, E corresponds to the elastic modulus of the substrate, ν denotes Poisson's ratio of the substrate and h and t are the thickness of the substrate and film, respectively.

The apparatus described in this article can directly provide curvature data without the need to measure bow height. For stress measurements during rapid thermal processing (RTP), curvature data can be acquired in 30 ms or even less. Thus, the study of the time-dependent material properties of metallic thin films in the plastic deformation regime shall particularly benefit from this apparatus. Additionally, the scanning mode of the multiple laser beams allows us to globally study the wafer curvature along the diameter of the wafer at each stabilized temperature. Eventually, the wafer bow data can be obtained by the extrapolation of curvature data. The RTP chamber is capable of creating a thermal environment from $-65\ ^{\circ}$C up to 650 $^{\circ}$C, which extends the temperature range of most of other tests [8–10] falling into the temperature range between room temperature and 500 $^{\circ}$C. As a result, the mechanical behavior of thin films at high temperatures and under cryo-conditions which are of great interest can be studied. Furthermore, an *in situ* formic acid treatment is also available for surface cleaning, which avoids the impact of unwanted oxidation and contamination on the investigated thin films.

2. Apparatus construction

The schematic diagram of the apparatus is shown in figure 1. The apparatus is composed of two main parts: a laser optics unit and a RTP chamber. The laser unit generates a multiple laser beam array which can be either scanned along the diameter of a wafer or used in a single position mode measuring a $1 \times 1\ \mathrm{cm^2}$ area at the center of the wafer. The RTP

chamber provides a thermal environment which is necessary for the investigation of thermal stress in thin films. The whole apparatus is fully controlled by the operational computer and software in the RTP heating module.

2.1. Optics

The laser beam array is created using a fiber-coupled laser diode (∼25 mW output, 660 nm wavelength) and a pair of etalon optics. The first etalon generates a linear array in the horizontal direction and the second etalon produces a two-dimensional array from the linear array. A beam splitter and 45° folder mirror send the array of parallel laser beams through a view port into the RTP chamber at normal incidence. The beams reflect off the wafer and back to the folder mirror, the beam splitter and a servo-controlled steering mirror. The servo mirror keeps the array centered onto a CCD camera. The wafer curvature is detected by the position of the multiple laser spots on the CCD detector. Since the data acquisition rate is rapid (approximately 0.07 s per data point), multiple measurements can be acquired so that the signal can be averaged over multiple measurements. In general, by averaging N points, the noise is reduced by a factor of $\sqrt{N}$. So averaging 25 points, for instance, reduces the error on the average value of the beam spacing by a factor of 5. The laser beam array provides two advantages: (i) wafer curvature can be measured instantly at any position of the wafer diameter, which guarantees the data accuracy at high ramp rate, e.g. 60 °C min^{-1} and (ii) vibrational noise can be effectively reduced by the subtraction of individual spot positions in the multi-beam array [11, 12].

2.2. RTP heating module

The RTP chamber equipped with the multi-laser optics mentioned above hosts the measurement of the wafer curvature. It has a front mounted slide door which is sealed by an O-ring. There is a 10 mm × 200 mm slit flange viewport on the top of the chamber to facilitate laser scanning and irradiation. The RTP chamber is an integrated system with a water-cooled aluminum main chamber, vacuum compatible quartz lined sample compartment, and three-point 200 mm quartz sample mount with an integrated thermocouple (type K) in contact with the sample surface. To ensure that the chamber wall remains cool, the chamber is surrounded by a highly polished and highly reflective water-cooled aluminum jacket. A diaphragm pump is used to provide a base pressure of ∼10 mbar for the chamber. Heating is performed with a sealed 12 × 12 crossed quartz lamp array, which can heat non-transparent samples up to 650 °C in a vacuum or gas environment of N_2 or forming gas (5% or 10% H_2 in N_2). The RTP chamber is also equipped with a liquid nitrogen heat exchanger, providing cold N_2 gas for active cooling. Consequently, it is capable of cooling from high temperatures down to −65 °C with a relatively high cooling rate (∼30 °C min^{-1}). Moreover, the system is equipped with a formic acid module which provides effective surface cleaning for wafer samples prior to the measurements.

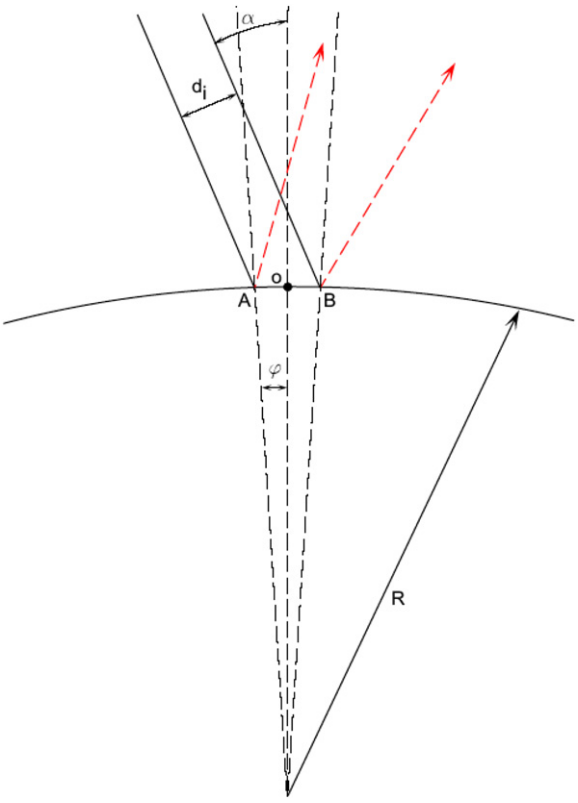

Figure 2. Two parallel laser beams strike on and reflect off a curved surface.

3. Performance of the apparatus

3.1. The principle of obtaining the curvature

Stress in a thin film is related to the curvature of the substrate through Stoney's equation. Thus, the key to the stress measurement is to obtain a precise measurement of the curvature. During the measurement, the sample is illuminated by an array of parallel laser beams, and the spacing of the reflected beams from the sample surface is determined by a CCD camera. The equation of curvature in relation to the spacing of the beams can be derived as follows. We assumed a wafer with a convex curvature with bending that occurs around center 'o', symmetric with two parallel incident beams as shown in figure 2. The true beam spacing is given by d_i, α is the angle of incidence, R is the radius of the sample and φ is the angle of the normal to the surface at the reflection point of the laser beams.

The distance between points A and B is given by

$$\text{AB} = \frac{d_i}{\cos\alpha} \tag{3}$$

and the angle φ is given by the following relation:

$$\sin\varphi = \frac{\text{AB}}{2R} = \frac{d_i}{2R\cos\alpha}. \tag{4}$$

Note that simple reflection requires that the angle between the two reflected beams be 4φ.

For complete generality, it is assumed that the substrate has an initial radius of curvature R_i. This is the case in which the initial curvature of the wafer is used as a reference for

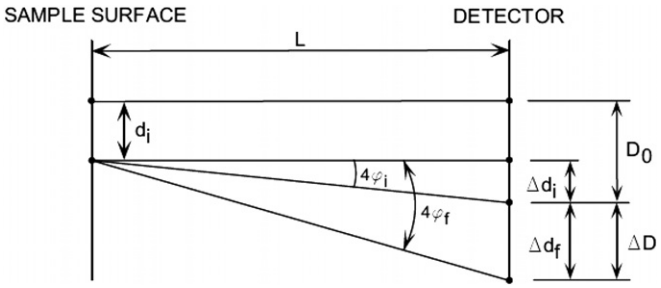

Figure 3. Reflected laser beams from the sample surface are detected by a CCD camera.

all subsequent curvature measurements. This initial curvature will cause the parallel laser beams to deflect with an angular deviation $4\varphi_i$, and the resulting change in beam spacing at the detector will be given by

$$\Delta d_i = L\tan(4\varphi_i) = L\tan\left(4\sin^{-1}\left(\frac{d_i}{2R_i\cos\alpha}\right)\right), \quad (5)$$

where L is the distance from the sample to the detector. As shown in figure 3, the reference spacing D_0 is now $d_i + \Delta d_i$. Any subsequent changes in curvature will be in addition to the initial substrate curvature and the total change in beam separation at the detector will be given by

$$\Delta d_i + \Delta d_f = L\tan(4\varphi_f) = L\tan\left(4\sin^{-1}\left(\frac{d_i}{2R_f\cos\alpha}\right)\right). \quad (6)$$

Δd_f can be found by subtracting equation (6) from equation (5). For approximation we can evaluate the product $\frac{d_i}{2R\cos\alpha}$ for the case of a maximum beam spacing of 8 mm and a small radius of curvature, such as 4 m. In this case, $\frac{d_i}{2R\cos\alpha}$ is about 0.001. Even for $\alpha \sim 60^\circ$, $\sin(x) = x$ is accurate to 2 ppm and $\tan(4x)$ is accurate to 5 ppm. Therefore, we can approximate and write

$$\Delta d_f = \frac{2Ld_i}{\cos\alpha}\left(\frac{1}{R_f} - \frac{1}{R_i}\right). \quad (7)$$

Finally, the relation between the change in laser spot spacing and the change in curvature of the sample is derived as

$$\frac{\Delta d_f}{d_i} = \frac{2L}{\cos\alpha}\left(\frac{1}{R_f} - \frac{1}{R_i}\right). \quad (8)$$

3.2. Measurement and resolution of beam spacing

The CCD detector used in the optics head is an 8-bit analog detector manufactured by Hitachi, model KP-M1AN. The detector uses a 2/3-inch format CCD with 768 × 474 active pixels with a pixel pitch of 11.64 (H) × 13.5 (V) μm. The output of the camera is the standard EIA video format, 30 frames s^{-1}. The detector has a built-in electronic shutter that has been set to 1/250 s to minimize the smear of the laser spots from sample vibration. The analog signal is digitized to the resolution of 640 × 484 using a PCI bus analog frame grabber, model PXR800 from CyberOptics Semiconductor.

The number of spots and the spacing between spots in the laser array can be configured by the rotation of the etalon optics. This system is configured with a 4 × 3 laser array which works well with the 4/3 aspect ratio of the 640 × 484 digitized image. The full width half maximum of a single laser beam within the array is typically around 13 pixels or approximately 180 μm.

The resolution of the system depends on how accurately the position of each laser spot can be determined. To determine the position, a centroid calculation is used which is similar to a 'center of mass' calculation but using intensity instead of mass. This provides a floating point position for each laser spot and is reproducible to 0.01 pixel if the system is isolated from vibration and temperature stabilized. Of course in most measurement applications, there are instabilities such as sample vibration caused by vacuum pumps and gas flow, as well as temperature non-uniformities that all affect the beam positions and thus reduce the reproducibility of the individual beam centroids.

The advantage of the multiple beam array technique is that it does not depend on the absolute position of a single beam. In optical techniques that use a single beam rastered across the surface, the measured position of the beam changes due to vibration of the sample, and this noise can significantly decrease the resolution of the curvature measurement. By using multiple parallel beam illumination, all the beams strike the surface at the same time. The differential beam spacing (i.e. the difference in the positions of adjacent beams that is used to calculate the curvature) is much less sensitive to the sample vibration than the absolute position of the beam. For example, the data in figure 4 show a case in which two individual beams oscillate in position due to a vibration of the sample. The change in the position of each individual beam centroid is quite large and oscillates at a consistent frequency. When the two individual beam positions are subtracted, the oscillation is effectively removed and the variability in the measurement is greatly reduced. The methods used in other instruments including single beam scanning and Shack–Hartmann sensors rely on measuring single beam positions. Although the Shack–Hartmann technique creates a multiple spot array by focusing local wave fronts to individual spots, the curvature calculation is based on the change in the position of each individual spot. The technique is still very susceptible to vibration.

3.3. Repeatability of single position and scanning measurements on 200 mm wafers

The repeatability of single point measurements was tested at room temperature with a ~723 μm thick bare Si wafer of ~200 mm diameter, polished on both sides. The curvature variation measured at the wafer center over a 60 s period is represented in figure 5. The corresponding theoretical stress changes for a 723 μm thick Si wafer deposited with a hypothetical film of 20 μm thickness are also presented. The plot reveals a background noise in the order of ±0.25 MPa.

The repeatability of the laser array scanning was then tested using a step size 5 mm and repeating the scan ten times along the wafer diameter. Thereby, the 2D wafer profile according to a horizontal reference plane is displayed in

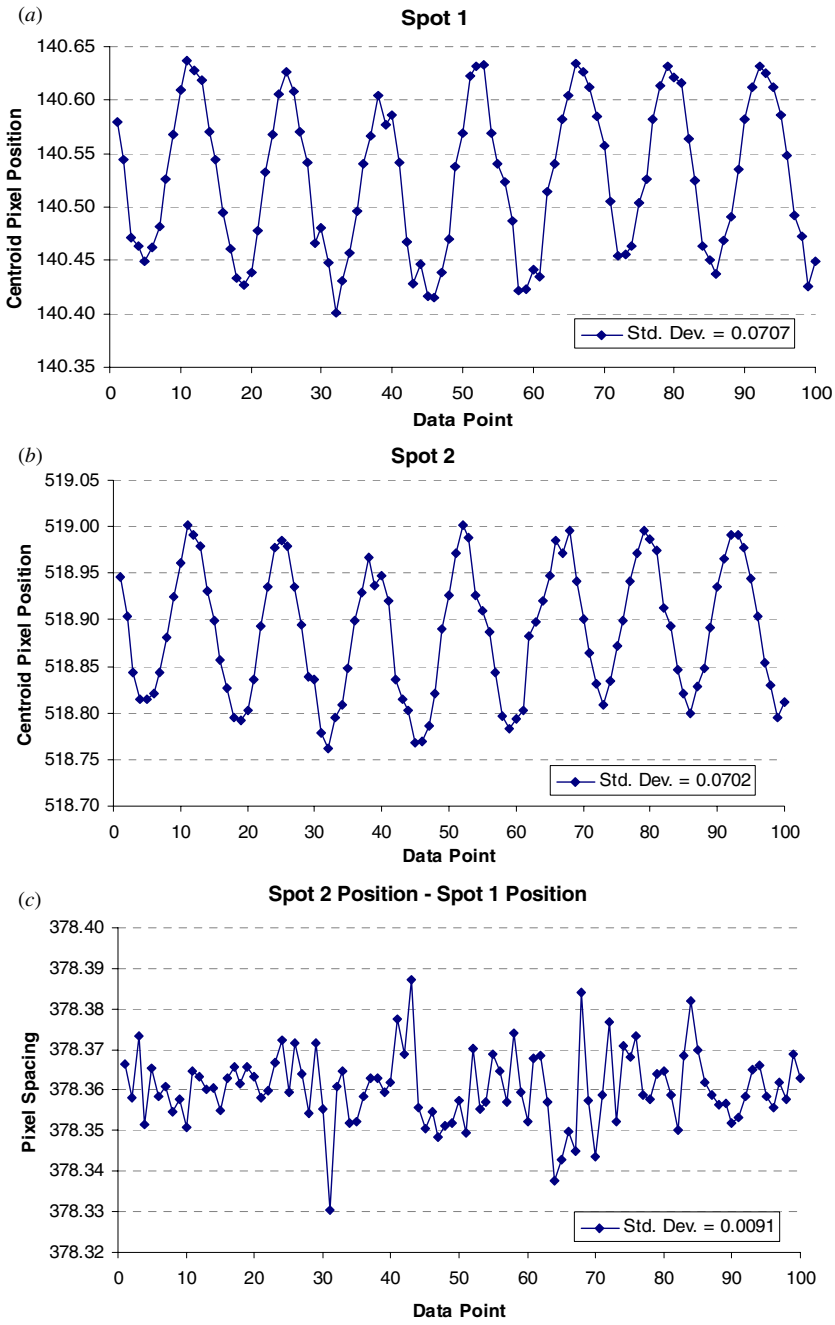

Figure 4. The reduction in vibrational noise by detecting the spacing change between parallel laser beams instead of the position change of a single laser beam. (*a*), (*b*) The position of two individual single laser beams; (*c*) the spacing between those two individual single laser beams which is the subtraction of the absolute positions of two single beams.

figure 6 to verify the signal repeatability of the scanning mode. The graph indicates that the wafer height curves mostly overlap each other and the maximum deviation is in the order of ± 0.10 μm.

3.4. Evaluation of temperature measurement

The measurement accuracy during a thermal cycle is not only determined by the curvature measurement but also by the accuracy of the temperature measurement with a thermocouple in contact with the wafer surface. The calibration of temperature measurement was performed in the temperature range between -65 °C and 650 °C with two wafers instrumented with thermocouples, a blank Si wafer and an equivalent Si wafer deposited with a 20 μm Cu film. The blank Si wafer was $\sim$200 mm in diameter with thickness of $\sim$723 μm, polished on both sides. The 20 μm thick Cu film was produced by electro-chemical deposition (ECD). Prior to that, a 100 nm thick thermal oxide was deposited by chemical vapor deposition (CVD) on the blank Si wafer as a diffusion barrier layer. Subsequently, a 50 nm thick Ti film was deposited as an adhesion layer, followed by a 150 nm thick Cu sputter-deposited seed layer. Near the center of the wafers, the system thermocouple (type K) is placed with

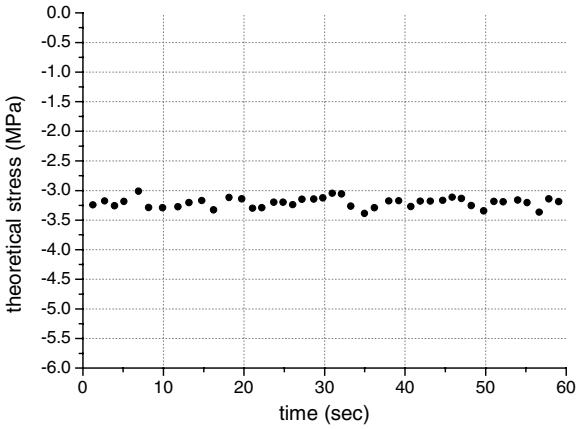

Figure 5. Repeatability of the irradiation of multiple laser beams at room temperature, tested with an 8″ blank Si wafer (∼723 μm). The theoretical stress is calculated according to the mentioned Si wafer deposited with a hypothetical film with 20 μm thickness.

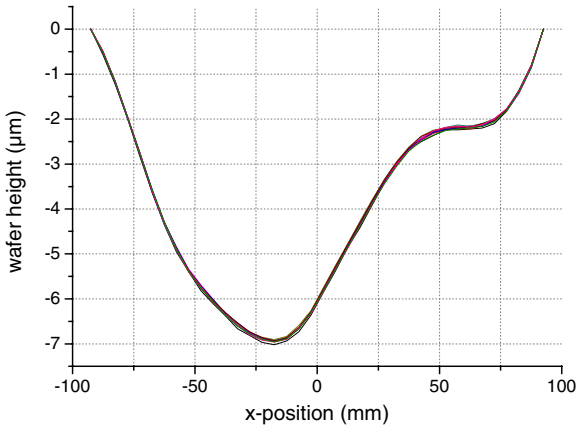

Figure 6. Repeatability of the scanning of multiple laser beams at room temperature, tested with an 8″ blank Si wafer (∼723 μm) ten times. The wafer height according to a horizontal reference ($y = 0$) is calculated based on the measured curvature data.

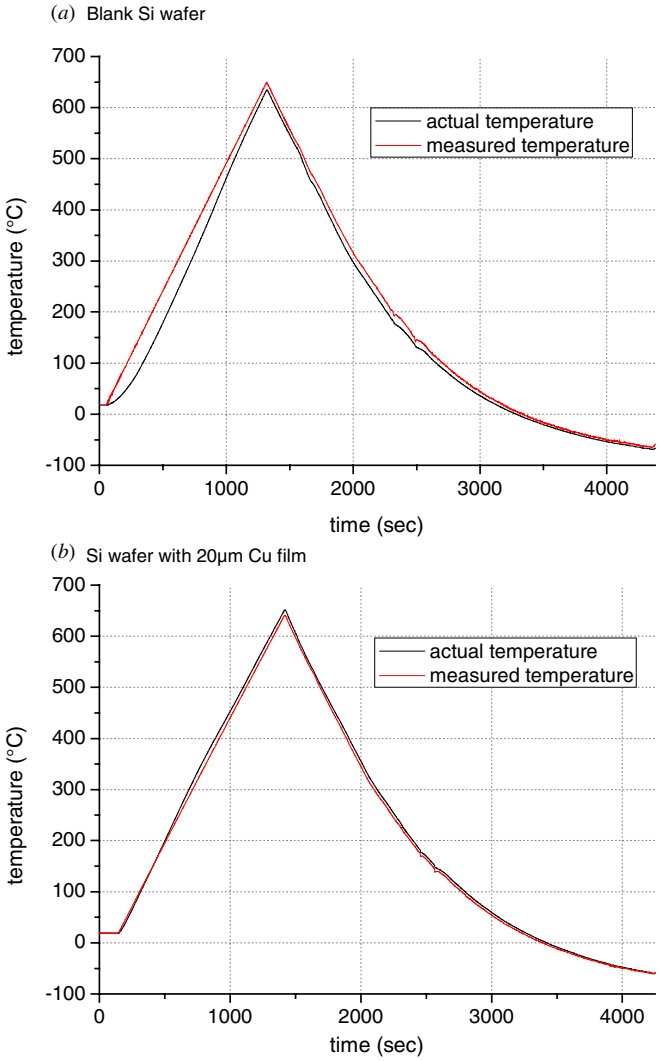

Figure 7. The actual temperature in comparison with the measured temperature during a thermal cycle from room temperature up to 650 °C with a ramp rate of 30 °C min^{-1}, then down to −65 °C. (*a*) Blank Si wafer; (*b*) Si wafer deposited with a 20 μm thick Cu film.

slight pressure contact to the surface. Another thermocouple is also bonded by a laser welding technique near the system thermocouple. Due to the better contact between the bonded thermocouple and the wafer surface, it is believed that the bonded thermocouple provides a more accurate measure of the sample temperature than the system thermocouple. The wafer is placed on the support pins in the quartz chamber in such a way that both bonded and system thermocouples are on the top side of the wafer, facing away from the heater lamps.

The results of the temperature measurement shown in figure 7 are quite different between the bare Si wafer and Cu film-coated wafer. For the bare Si wafer (see figure 7(*a*)), the measured temperature from the system thermocouple is always higher than the actual wafer temperature which is determined by the bonded thermocouple during the entire cycle. The maximum temperature deviation occurs at ∼100 °C during heating. Subsequently, the deviation reduces with increasing temperature. During cooling, the temperature deviation stays nearly constant until ∼100 °C, at which point the temperature deviation becomes smaller due to the significantly slower cooling rate. In comparison, the deviation between measured and actual wafer temperature is considerably reduced for the Cu film-coated wafer for the entire cycle (see figure 7(*b*)). Only during the heating above 250 °C is the measured temperature a bit lower than the actual one.

As the temperature of silicon wafer increases, the band gap decreases and the wafer becomes increasingly absorbing of the infrared radiation from the lamp heater [13, 14]. Consequently, the thermocouple wires behind the silicon wafer absorb less infrared radiation and more accurately track the true wafer temperature. This leads to the observation that the measured temperature is remarkably higher than the actual wafer temperature for the bare Si wafer at low temperatures and during rapid temperature ramping. On the other hand, if a Cu film is deposited on the Si wafer, the infrared radiation is effectively blocked from the thermocouple wires and most of the infrared is absorbed by the Cu film. Therefore, the temperature deviation can be reduced practically by the Cu

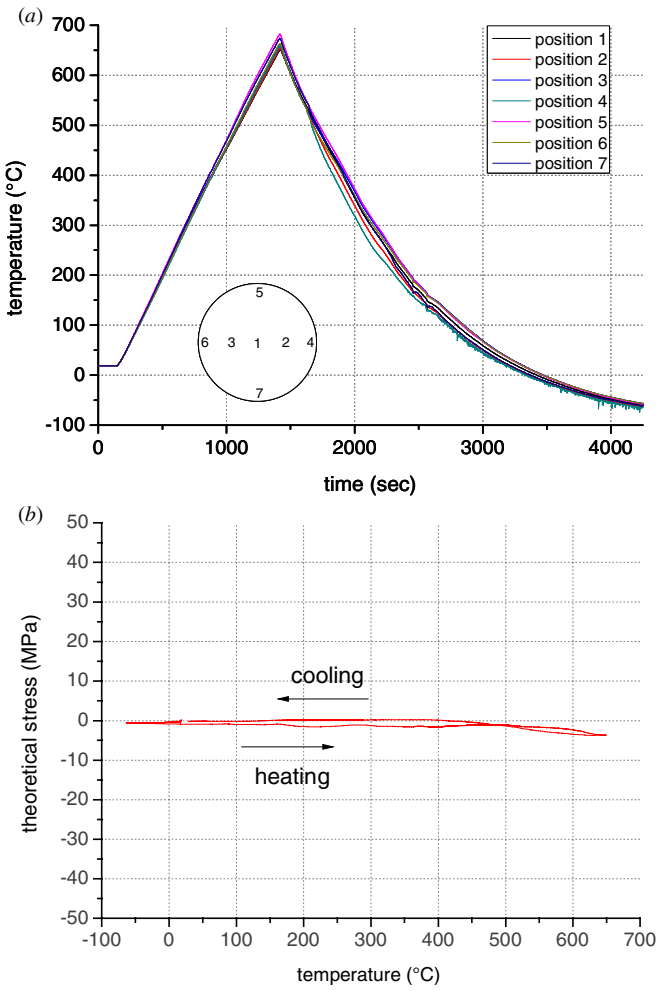

Figure 8. Thermal uniformity on a blank Si wafer with a thickness of 723 μm during a thermal cycle with a ramp rate of 30 °C min^{-1}. (*a*) Thermal profiles of seven temperature sensors at different positions of the sample surface. (*b*) Evolution of the theoretical stress during the thermal cycle. The theoretical stress refers to the biaxial stress of a hypothetical film of 20 μm thickness deposited on a 723 μm thick Si wafer.

film. This substantiates that temperature calibrations based on a bare Si wafer for thermal stress measurements of metallic films could be misleading.

3.5. Temperature uniformity of RTP chamber

The temperature uniformity on a sample wafer is of high importance especially when the ramping rate is high, because temperature non-uniformity will lead to an unwanted thermally induced wafer curvature. Therefore, the same type of blank Si wafer as mentioned above was equipped with seven temperature sensors (see figure 8(*a*)), which are bonded at the center (position 1), at ∼75 mm distance from the center (positions 2, 3) and at ∼100 mm distance from the center (positions 4–7), respectively, and were used to measure the temperatures at different locations on the wafer surface. The sensor bonding method is the same as mentioned in section 3.2.

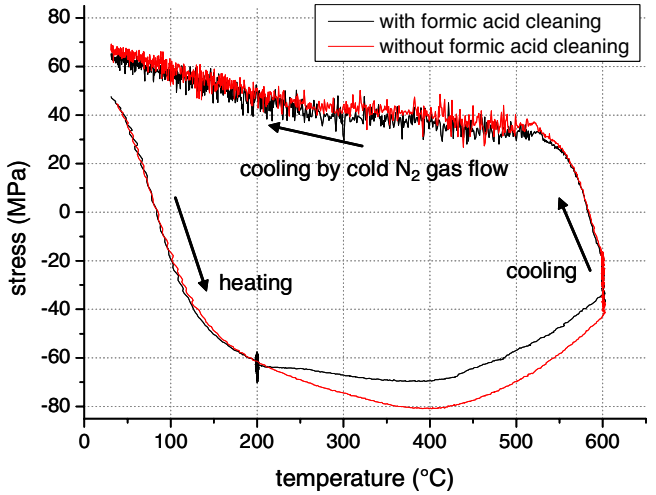

Figure 9. Stress hysteresis of 20 μm thick Cu film during a thermal cycle between room temperature and 600 °C with a ramp rate of 30 °C min^{-1}. The measurement noise below ∼500 °C during cooling is induced by the large volume of cold N_2 gas flow. The disparate tendency of two stress hysteresis curves is caused by the removal of native oxide on the Cu film applying a formic acid treatment at 200 °C for 10 min.

The temperature profiles of each temperature sensor during a thermal cycle (−65 °C to 650 °C) are plotted in figure 8(*a*), which indicates that the temperature uniformity is disturbed above 500 °C during heating and below 500 °C during cooling. This observation corresponds well to the calculated theoretical stress based on the wafer curvature recorded during the thermal cycle, which is shown in figure 8(*b*). The relatively good temperature uniformity up to ∼500 °C leads to a plateau of the theoretical stress. Explicitly, no distinct curvature is generated by the thermal non-uniformity at this phase. However, the theoretical stress starts to change above 500 °C, which is in agreement with the disparate tendency of the temperature profiles of seven sensors. In order to keep a high cooling rate, the cold N_2 gas purges into the chamber below 500 °C with a massive flow. Understandably, the theoretical stress curve during active cooling diverges from the one during heating because of the disturbed temperature uniformity. Below 100 °C, the stress curve converges with the one during heating because of the improved temperature uniformity by a relatively slower cooling rate.

There are two points one must be aware of. First of all, the significant change of theoretical stress above ∼500 °C may not only originate from the reduced temperature uniformity, but also be induced by the thermal gradient from the lamp heated side of the sample to the unheated side [11]. Unfortunately, due to the fact that the temperature difference between two wafer sides is unknown, it is difficult to estimate the magnitude of the effect from thermal gradient. Secondly, a Si wafer coated with a Cu film should achieve better thermal uniformity because of the high heat conductivity of copper.

4. Test results on Cu films

Cu film is easily oxidized in the ambient atmosphere. Depending on the exposure time and temperature, the

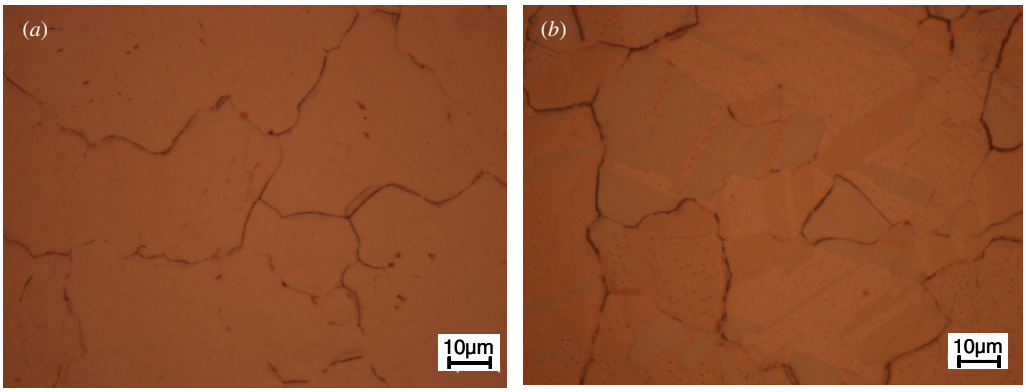

Figure 10. Optical microscopic images of the surface of 20 μm thick Cu films: (*a*) without formic acid treatment; (*b*) with formic acid treatment at 200 °C for 10 min.

thickness of native oxide layer on Cu films can be up to several tenths of a nanometer [15, 16]. The cleaning treatment to remove the native oxide influences the thermo-mechanical behavior of the Cu film especially at high temperature because the oxide layer may act as a passivation layer for the Cu film. The stress hysteresis of a 20 μm thick Cu film with and without formic acid cleaning is shown in figure 9. A significant difference in the film stress evolution is observed between the sample treated with *in situ* formic acid cleaning at 200 °C and the one without cleaning treatment. Meanwhile, it is observed in figure 10 that more grain grooves, boundaries and twins can be seen on the surface of the Cu film after formic acid treatment. It is believed that *in situ* acid treatment helps to remove native oxide; thus, the diffusion path via grain boundaries to the free surface is no longer blocked. Therefore, a reduced compressive stress is expected as shown in figure 9 at a high temperature range because the stronger stress relaxation mechanism such as diffusion is effectively activated.

5. Conclusions

In this paper, a novel apparatus for measuring local stress of thin films by an array of parallel laser beams has been proposed. The measurements can be performed not only at room temperature but also at elevated temperatures and under cryo-conditions. The evaluation tests demonstrate that the vibrational noise can be reduced more than ten times by using an array of parallel laser beams instead of single laser beam scanning. As a result, the resolution of curvature measurements is largely improved. Furthermore, due to the fast data acquisition (<30 ms) the local stress measurement during the rapid thermal processing becomes reliable, from which the study of time-dependent material properties will benefit. Additionally, the evaluation tests also prove that new insights into material behavior and thin film properties can be discovered by the effective *in situ* sample cleaning which is integrated in the apparatus.

Acknowledgments

The authors would like to thank M Schneegans, P Nelle, R Thomson and T Bitzer for the fruitful discussions. This work was jointly funded by the Federal Ministry of Economics and Labor of the Republic of Austria (contract 98.362/0112-C1/10/2005) and the Carinthian Economic Promotion Fund (KWF) (contract 18911 | 13628 | 19100).

References

[1] Mishnaevsky L L Jr and Gross D 2005 Deformation and failure in thin films/substrate systems: methods of theoretical analysis *Appl. Mech. Rev.* **58** 338
[2] Nix W D 1989 Mechanical properties of thin films *Metall. Trans.* A **20** 2217–45
[3] Freund L B and Suresh S 2003 *Thin Film Materials: Stress, Defect Formation, and Surface Evolution* (Cambridge: Cambridge University Press)
[4] Segmüller A, Angilelo J and La Placa S J 1980 Automatic x-ray diffraction measurement of the lattice curvature of substrate wafers for the determination of linear strain patterns *J. Appl. Phys.* **51** 6224
[5] Chen K S, Chen T Y F, Chuang C C and Lin I K 2004 Full-field wafer level thin film stress measurement by phase-stepping shadow moiré *IEEE Trans. Compon. Packag.* **27** 594–601
[6] Grédiac M 2004 The use of full-field measurement methods in composite material characterization: interest and limitations *Composites* A **35** 751–61
[7] Doerner M F and Nix W D 1988 Stresses and deformation processes in thin films on substrates *Crit. Rev. Solid State Mater. Sci.* **14** 225–68
[8] Chocyk D, Proszynski A and Gladyszewski G 2008 Diffusional creep induced stress relaxation in thin Cu films on silicon *Microelectron. Eng.* **85** 2179–82
[9] Mann A B, Tapson J, Heerden D v, Lewis A C, Josell D and Weihs T P 2002 Apparatus to measure wafer curvature for multilayer systems in a vacuum furnace *Rev. Sci. Instrum.* **73** 1821–7
[10] Weihnacht V, Bruckner W and Schneider C M 2000 Apparatus for thin-film stress measurement with integrated four-point bending equipment: performance and results on Cu films *Rev. Sci. Instrum.* **71** 4479–82

[11] Floro J A and Chason E 2001 *Curvature-Based Techniques for Real-Time Stress Measurement During Thin-Film Growth* (New York: Wiley-Interscience) p 191
[12] Chason E H, Floro J A, Seager C H and Sinclair M B 1999 Measurement of the curvature of a surface using parallel light beams *US Patent* 5912738
[13] Dash W C and Newman R 1955 Intrinsic optical absorption in single-crystal germanium and silicon at 77 K and 300 K *Phys. Rev.* **99** 1151–5
[14] Moss T S 1959 *Optical Properties of Semi-Conductors* (London: Butterworths Scientific Publications)
[15] Chu Y S, Robinson I K and Gewirth A A 1999 Comparison of aqueous and native oxide formation on Cu (111) *J. Chem. Phys.* **110** 5952
[16] Hu Y Z, Sharangpani R and Tay S P 2001 *In situ* rapid thermal oxidation and reduction of copper thin films and their applications in ultralarge scale integration *J. Electrochem. Soc.* **148** G669